

Development of a Grain-Scale Model for Shock Initiation of HNS

David L. Damm¹, Ryan R. Wixom², and Cole D. Yarrington²

1. Schlumberger Technology Corporation, Houston, TX, USA
 2. Sandia National Laboratories, Albuquerque, NM USA

Abstract. The shock initiation of energetic materials is governed by the release of chemical energy at hotspots which are created by localization of the shock wave energy at discontinuities or defects in the material. We have conducted numerical simulations of the shock-to-detonation transition in porous beds of granular hexanitrostilbene (HNS) using realistic microstructures, a first-principles equation of state, and local temperature-dependent homogeneous reaction kinetics. The model geometry consists of a solid matrix of crystalline HNS with discrete cylindrical pores or voids whose size distribution and placement is statistically equivalent to the observed microstructure in cross-sectioned samples of HNS. The equation of state for the solid phase was derived from density functional theory molecular dynamics (DFT-MD) calculations of the Hugoniot for crystalline HNS. In typical simulations the bed is impacted by a thin flying plate which drives a shock wave into the material. The shock wave compresses the solid and crushes the voids thus creating localized regions whose temperature and pressure exceed the bulk average. In addition, the release of chemical energy at these hotspots creates a reactive flow field which is highly non-uniform in both pressure and temperature. The flow field either builds up to detonation conditions or is quenched by release waves depending on the magnitude of the impact shock, duration of the impact shock, porosity of the bed, and pore size distribution within the bed. The temperature predictions for the solid phase have been improved by implementing a temperature-dependent specific heat, and by accounting for heat generation due to plastic work or yielding of the material. The dependence of the local temperature fields on initial void geometry has also been analyzed. These results are aiding in the development of grain-scale simulations which strike a balance between accuracy and computational expense.

Introduction

Continuum reactive burn models are widely used in hydrocodes for numerical simulation of the shock-to-detonation transition in heterogeneous energetic materials. Properly calibrated burn models provide satisfactory performance in many applications, provided that the continuum approximation is valid for the problem at hand. In some cases, this approximation becomes poor. For

example, if the duration of the incident shock pulse is very short (relative to the size of microstructural features), then the continuum approximation may give poor results. Similarly, if the size of volume elements within the computational mesh are approaching the length scale of microstructural features, then the computational domain is not truly a continuum.

In heterogeneous materials, the initiation of chemical reactions is believed to occur at defects

such as voids, cracks, grain boundaries, or any other discontinuity where local temperature and pressure can far exceed the bulk average. Non-continuum (or so-called “mesoscale”) models have provided insight into how these heterogeneities localize the shock energy and create local conditions which are favorable for the onset of reactions. Throughout the years, models of varying complexity have been developed ranging from simple geometries such as single spherical voids^{1,2} to highly detailed geometries including large ensembles of neat³ or plastic-bonded⁴ explosive grains. Those simulations have typically been limited to unit cells or representative volume elements which capture the statistical behavior of the shock response of the bed, but are inadequate to directly simulate the complete transition to detonation.

Direct numerical simulation of shock initiation of heterogeneous materials has significant practical application. For example, it is a tool which could be used to calibrate continuum burn models while explicitly accounting for heterogeneities in the sample. At present, continuum burn models are calibrated with data from heterogeneous samples, thus the parameters are not sample independent. The same explosive, pressed to a different density, or from a different batch of powder likely requires a different set of reactive burn model parameters. Thus there is significant motivation to develop and validate grain-scale models which explicitly include the microstructure of the material.

Here we present the recent development⁵ of a grain-scale model which has successfully simulated the growth to detonation (or failure) of shock waves in pressed beds of granular hexanitrostilbene (HNS) using homogeneous local reaction kinetics and discrete microstructures. After a brief review of this modeling framework and simulation results, we discuss refinement of the model including the implementation of a new tabular EOS for unreacted HNS, the role of material strength during void collapse, and the effects of void shape and orientation on hot spot temperature.

Model Description

The 2D model geometry consists of a solid matrix of pure HNS with discrete circular pores or voids whose size distribution is statistically equivalent to the void size distribution which has been measured in cross-sectioned samples of compacted HNS powder⁶. Fig. 1 shows an example of a binarized micrograph of a real cross-section and an equivalent simulated cross-section which forms the basis of the model geometry. Each void in the SEM image was fit by an equivalent circular void. The void diameter distributions for various samples were fit by log-normal curves with the mean ranging from 136–254 nm.

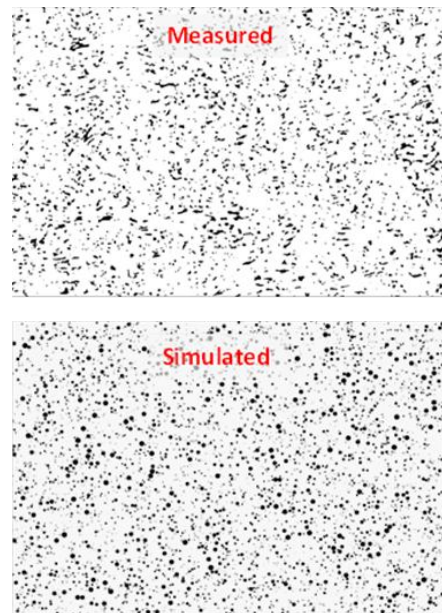


Fig. 1. Binarized image of pellet cross-section (top) and simulated microstructure with circular voids (bottom).

While the resolution of the SEM is quite high (several nm), the resolution of the micrograph shown in Fig. 1 is only 24.4 nm/pixel (25000 nm field of width recorded onto 1024 pixels). Considering the image resolution and practical limitations for computational mesh resolution, voids less than 20 nm in diameter were not included when generating the simulated microstructure from the functional form of the

measured distribution. It is interesting to note that the size of the unit cell for a molecule of HNS is approximately 1 nm—a limit below which the material is clearly not a continuum.

The equation of state for the solid phase was derived from density functional theory molecular dynamics (DFT-MD) calculations of the Hugoniot for crystalline HNS⁷. The DFT-MD predictions were fit by a second order polynomial,

$$U_s = 2.761 + 1.853u_p - 0.1125u_p^2 \quad (1)$$

Where U_s is the shock velocity and u_p is the material velocity. Although additional calculations are underway, points on the Hugoniot have only been calculated up to a pressure of 32 GPa, so caution is recommended if using Eq. (1) at higher pressures. The equation for the Hugoniot of crystal-density HNS was implemented in CTH using the Mie-Gruneisen analytical option.

The porous bed was impacted at the lower horizontal boundary by a plate traveling at a velocity of several km/s. Periodic boundary conditions were applied to the vertical boundaries. The top horizontal boundary was treated as a semi-infinite medium. At high impact velocities—those required for detonation—the impact stress exceeds the yield stress of the material by an order of magnitude or more. Therefore strength of the solid was neglected in our preliminary calculations. (This assumption was subsequently relaxed and the results are discussed below.)

The rate of conversion of HNS to its reaction products is described by the following relationship,

$$d\lambda/dt = (1 - \lambda)A\exp[-E_a/T] \quad (2)$$

where λ is the extent of reaction, E_a is the activation energy, T is the temperature of the solid, and A is a constant. The activation energy is based on data for thermal decomposition of HNS⁸. For the state of the reaction products, a sesame table of states based on thermochemical equilibrium calculations⁹ was used here.

Simulation Results

Two-dimensional rectangular simulations were carried out in the shock-physics code, CTH. The porous bed is impacted by a thin flying plate which drives a shock wave into the material (see Fig. 2). The shock wave compresses the solid and crushes the voids, thus creating localized regions whose temperature and pressure far exceed the bulk average. When the rate of chemical energy release is greater than the dissipation of energy (due to rarefaction waves and/or thermal diffusion) the shock strength increases until steady detonation is achieved. Below this threshold, the shock wave weakens and fails to form into a steady detonation.

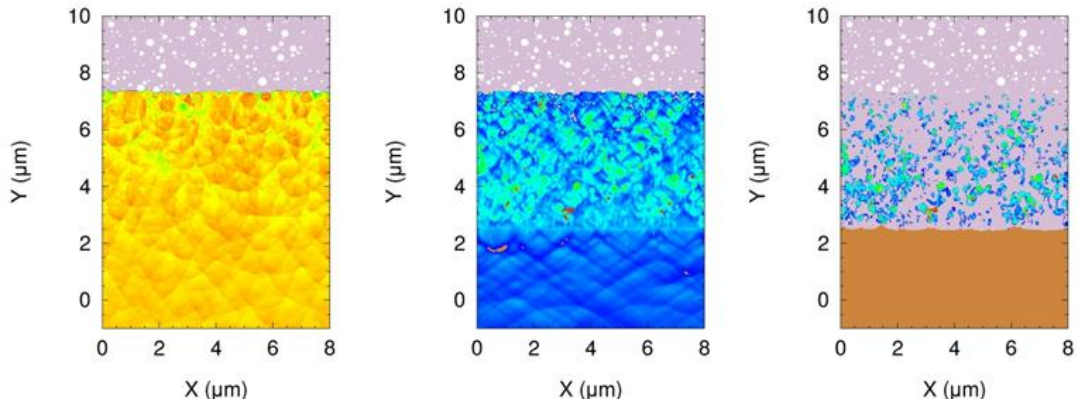


Fig. 2. Hydrocode simulations of plate impact into a porous bed of HNS. The colormaps show pressure, temperature, and extent-of-reaction profiles (left to right) 1.75 ns after impact. These simulations have been scaled up to accommodate run distances up to several hundred μm .

The simulation results capture the phenomenon of shock waves in a porous bed which either successfully run-up to detonation or fail to detonate—depending on the initial shock strength, porosity, and pore-size distribution. Fig. 2 shows a sample of pressure, temperature, and extent-of-reaction profiles within the porous matrix 1.75 nanoseconds after impact. The shock wave has traveled approximately 7 μm into the material and the compressed region shows noticeable evidence of hotspot formation and growth. Fig. 3 illustrates local pressures along a line placed 1 micron deep within the porous bed below the impact interface. The bulk average pressure at impact is approximately 10 GPa but local pressure variations exceeding 13 GPa and as low as 5 GPa are also observed. After a few nanoseconds the pressure drops rapidly as the release wave from the rear surface of the flyer arrives at the impact interface.

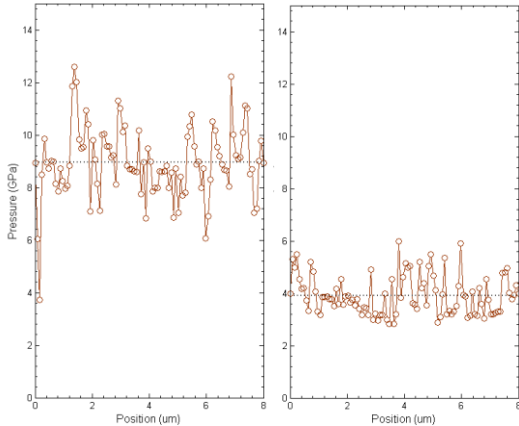


Fig. 3. Local pressure variations 1 um below the impact surface, 1ns (left) and 5ns (right) after impact.

The average pressure at various depths within the material is shown in Fig. 4. The pre-exponential factor in the reaction rate (Eq. 2) was adjusted such that the predicted threshold flyer velocity for successful run-up to detonation matches the experimentally measured velocity (~3200 m/s). At 3100 m/s, the shock wave initiates noticeable reactions and momentarily

grows—until the release wave from the rear surface of the flyer arrives and relieves the pressure. The average pressure starts to fall and the flow field never reaches detonation conditions. At 3200 m/s the impact shock is slightly stronger and the release wave is not able to overtake the shock front. The average shock strength builds up gradually then rapidly transitions to detonation at a depth of approximately 100 um.

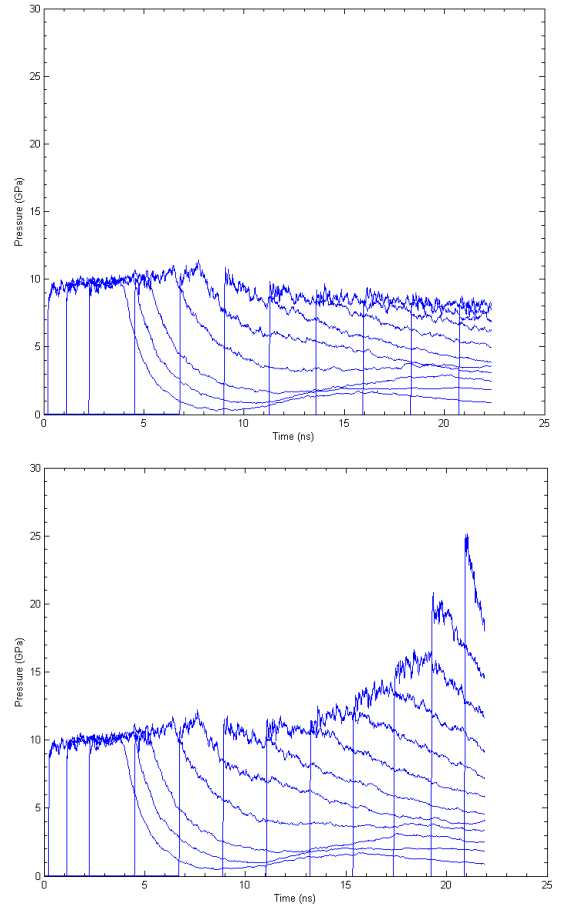


Fig. 4. Average pressure at depths of 1, 5, 10, 20...90 microns. The upper image shows failure to detonate following flyer impact at 3100 m/s. In the lower image, the shock wave transitions to detonation after flyer impact of 3200 m/s.

The simulation results exhibit features which are typical of shock initiation in heterogeneous

explosives—even though the reaction rate in this case is homogeneous. The heterogeneous behavior is a consequence of discontinuities in the microstructure which were explicitly modeled here. The relationship between void size and run distance to detonation was investigated with the simulation. As the void size increases, the run distance also increases because the voids are fewer and further apart (to maintain a constant density). However, it may be more appropriate to correlate the shift to longer run distances to the increase in the interface area (surface area of the voids). This relationship is shown in Fig. 5.

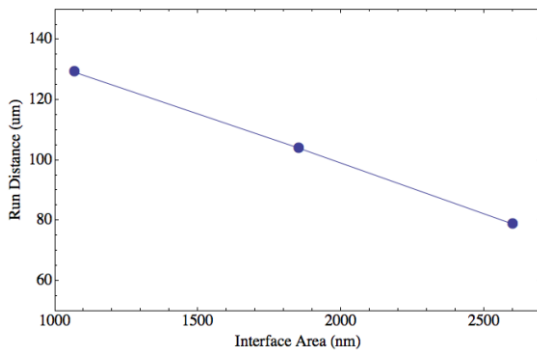


Fig. 5. Run distance to detonation for various interfacial surface area (3200 m/s impact velocity).

Of course, the interface area and circular void diameter are very simply related for uncomplicated geometrical shapes, but in real materials this isn't the case. Khasainov et al.¹⁰ compiled experimental evidence of this relationship for a variety of explosives showing clear linear trends of changing critical diameter and run distance with increasing interface area of both void and solid particle heterogeneities.

Model Refinement

A major source of error in the predicted temperature fields and reaction rates is the assumption of constant specific heat. In order to improve the accuracy of the model, we have implemented a recently-developed, tabular equation of state which includes a non-constant or temperature-dependent specific heat¹¹.

Fig. 6 compares the predicted temperature fields during void collapse using the constant specific heat EOS and the new sesame table with temperature-dependent specific heat. The initial shock pressure is 6 GPa and reactions are not included in this simulation. The predicted bulk average temperatures behind the shock wave are 507 and 443 K for the constant and variable specific heat cases, respectively. The maximum temperatures in the solid phase near the crushed void are 1803 and 1163 K, for the constant and variable specific heat cases, respectively. This significant discrepancy in predicted temperatures is amplified in the reaction rate due to its exponential dependence on temperature.

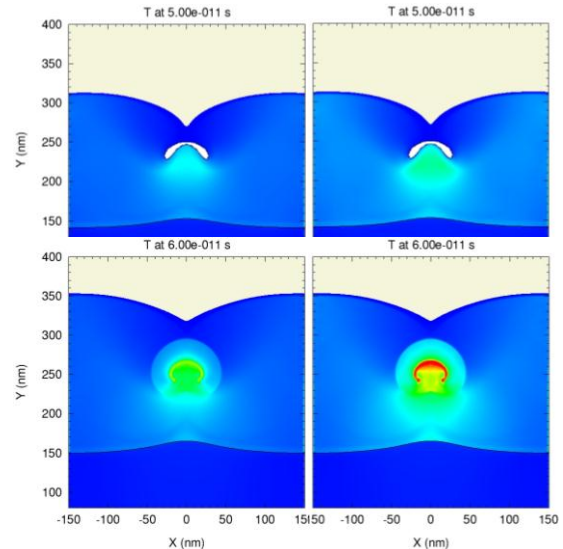


Fig. 6. Temperature of the solid HNS after pore collapse for the case of constant specific heat (right) and temperature-dependent specific heat (left). The temperature scale is from 300 to 1500 K.

The mechanical strength of the material also has a significant effect on the temperature of the solid during deformation. To investigate these effects, we applied the elastic-perfectly plastic model with various yield strengths ranging from 100-1000 MPa. The addition of material strength has two effects. First, the leading surface of the void does not form a jet and collapses with a reduced velocity as the yield strength increases

(see Fig. 7). Second, the temperature of the solid increases due to plastic deformation (in addition to the temperature increase caused by adiabatic compression). These effects start to become visibly noticeable for yield strengths of 100 MPa and greater. This is somewhat surprising because the impact stress in these simulations was 6 GPa (a factor of 60 times greater than the minimum yield strength). However, the results agree with previous works by Menikoff² and Khasainov¹² who included viscous effects in their calculations and showed that temperature of the solid during void collapse has a strong dependence on the viscosity. Menikoff further concluded that hydrodynamic void collapse was an insufficient mechanism to generate the temperatures necessary for hotspot ignition on the timescale necessary for shock initiation of HMX.

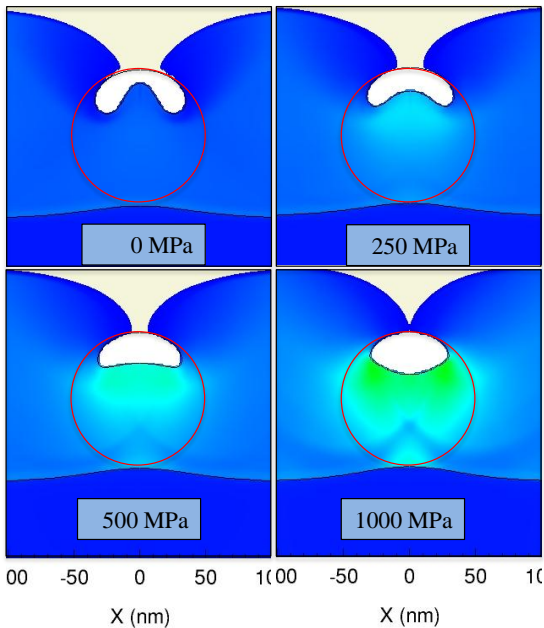


Fig. 7. Circular void partially compressed by a 6 GPa shock wave. The compressive yield strength for the elastic-plastic model is indicated in each frame. The simulation time is the same for each frame. The color indicates temperature, which ranges from 443 K behind the unperturbed shockwave to a maximum of 765 K in the lower right frame in the region of void closure.

The peak temperatures after void crushing are also heavily dependent on yield strength. Fig. 8 shows the maximum temperature of the solid as a function of elastic-plastic yield strength. The hydrodynamic case is represented by zero yield strength. The peak temperatures increase moderately up to 500 MPa with a dramatic increase observed at higher yield strengths. The dynamic compressive strength of crystalline HNS is not known; however it is likely to be in the same range as other explosives (for example, 100-300 MPa¹²). In this range, peak temperatures fall between 1030 and 1200 K—a relatively small window given the many assumptions of the present analysis and large uncertainty in material properties.

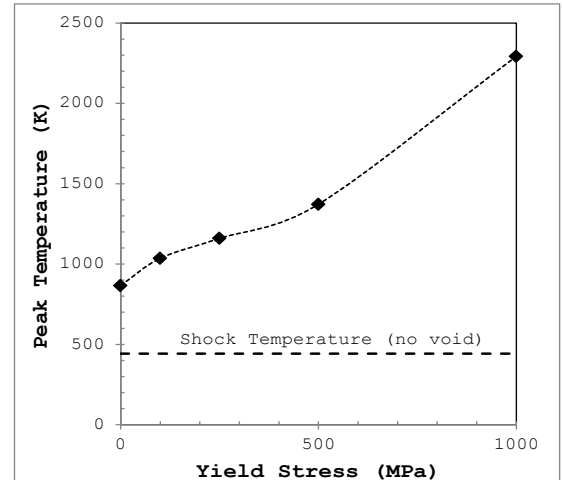


Fig. 8. Peak temperature of the solid during shock wave compression and void crushing. Zero yield stress represents the case of purely hydrodynamic flow.

The shape of the void also influences the temperature of the hotspot. Tarver¹³ assumed the existence of spherical, cylindrical, and flat plate (slab) hotspots, and used a 1-d thermal diffusion model coupled with a temperature-dependent reaction rate to calculate the critical temperature for ignition. As expected, the initial temperature required for hotspot ignition was greatest for the spherical hotspot, followed by cylindrical then slab geometries. The trend is governed by the rate of heat loss to the surroundings for the three shapes

considered. Here, we have specified an initial void shape (based on observations of voids in cross-sectioned material samples) and calculated the shape and temperature of the resulting hotspot. The initial shape of the void plays a significant role in the size of the heated region and the temperature increase that is generated.

Oblong voids oriented parallel and normal to the shock front were considered. The parallel-oriented void is analogous to the concept of a “slab” hotspot, however the temperature fields in the vicinity of the crushed void are highly irregular and non-planar (see Fig. 9). A small, intensely heated region is created at the vertical mid-plane of the void due to convergence of jets from the edges. Oblong voids which are normal to the shock front also create hotspots with complicated shapes. Both configurations of oblong voids generate temperature fields which look very different from each other and very different from those in Fig. 6. The temperature fields do not appear to follow an intuitive pattern and bear little resemblance to the initial void geometry.

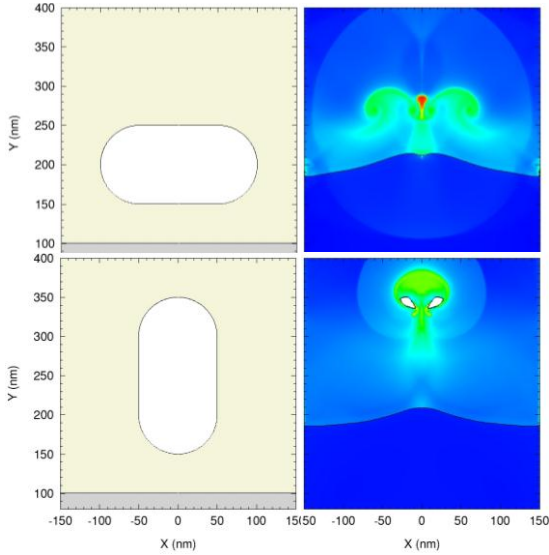


Fig. 9. Oblong voids oriented parallel (top) and normal (bottom) to the shockwave. The otherworldly temperature fields (shown 98 ps after impact) bear almost no resemblance to the initial void geometry. Reactions were not included in these calculations.

Real voids have a much more complicated geometry than the simplified cases considered above. Fig. 10 is an image of a cross-sectioned sample of pressed HNS illustrating the wide variety of shapes and sizes of voids which can be expected. One of these voids was extracted for simulation and the results are shown in Fig. 11. Again, the hotspot is rather unique, looking nothing like the original void geometry from which it was formed. We suspect that various orientations of this void with respect to the shock front will also yield varying results.

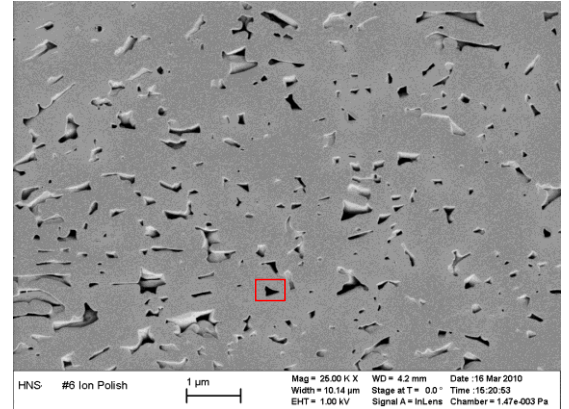


Fig. 10. Image of ion-polished HNS showing pore structure. The red square indicates the void which was extracted for the simulation.

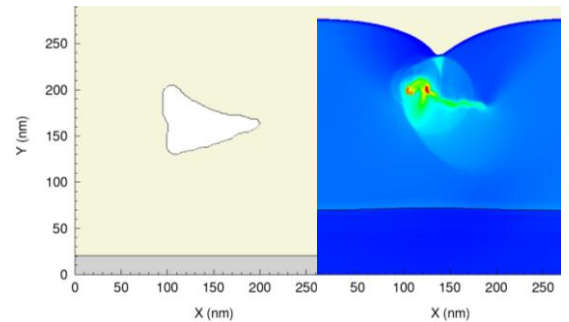


Fig. 11. Simulation of a void with actual geometry imported from the image in Fig. 10.

It is not practical to consider all possible pore geometries and orientations; thus it is imperative to identify statistically equivalent approximations

and treat the microstructure in a probabilistic manner similar to the methods employed by Baer¹⁴ or Barua¹⁵. The purpose of studying individual voids or defects is to identify satisfactory approximations to the literal microstructure such that *statistically* equivalent microstructures will yield *physically* equivalent results. Similarly, the best available physical models can be applied to simulations of single voids, in hopes of identifying satisfactory simplifying assumptions which make the large-scale simulations of many voids computationally feasible. Once this is achieved, direct numerical simulations of shock initiation in heterogeneous beds may be carried out and provide the information necessary for parameterization of continuum models.

Conclusions and Future Study

We have developed a model for the shock-to-detonation transition in porous beds of granular hexanitrostilbene (HNS) using realistic microstructures, a first-principles equation of state, and local temperature-dependent reaction kinetics. The initiation of reactions is governed by discontinuities in the microstructure (voids) which have been explicitly included in the model geometry. The model directly simulates the shockwave interaction with voids, local deformation and heating of the solid matrix, subsequent release of chemical energy, and progression of the reactive flow field to quasi-steady detonation conditions.

Several model refinements including temperature-dependent specific heat, material strength, and pore geometry were demonstrated for simulations of individual voids. These studies have illustrated several areas in which the accuracy of the model can be improved. First, the strength of the solid material at the micro-scale, under dynamic loading conditions is poorly understood. Our results showed that even the inclusion of a simple elastic-perfectly plastic model with relatively low yield strength can significantly affect the predicted temperature of the solid. This, in turn, directly affects the rate of chemical energy release. Refinement of the strength models is critical for achieving accurate predictions of temperature.

The second area for improvement is the reaction mechanisms which link the local thermodynamic conditions to the rate of chemical energy release. The kinetics may be more complicated than the single-step Arrhenius kinetic rate that was assumed here. We are currently investigating the shock-induced chemistry in HNS and other materials and plan to incorporate those results into this model as they become available.

A third topic for investigation is the validity of the continuum hydrocode at the sub-micron length scale. Large-scale reactive molecular dynamics simulations are approaching this length scale^{16,17} and may eventually overlap the lower end of the continuum. The ability to validate and parameterize the continuum models using molecular dynamics techniques would represent a major step forward in energetic materials research.

Despite these areas for improvements, the modeling approach presented here is a useful tool for studying the role of microstructure on the initiation behavior of heterogeneous explosives.

Acknowledgements

This work was supported in part by the Laboratory Directed Research and Development program and the Advanced Scientific Computing program at Sandia Labs. Sandia National Laboratories is a multi-program laboratory managed and operated by Sandia Corporation, a wholly owned subsidiary of Lockheed Martin Corporation, for the U.S. Department of Energy's National Nuclear Security Administration under contract DE-AC04-94AL85000.

References

1. Mader, C.L., *Numerical Modeling of Explosives and Propellants*, CRC Press, Boca Raton, FL 1998.
2. Menikoff, R., "Pore Collapse and Hotspots in HMX" Shock Compression of Condensed Matter – 2003, pp. 393-396
3. Gilbert, J., Chakravarthy, S., and Gonthier, K.A., "Computational Analysis of Hot-spot Formation by Quasi-steady Deformation Waves in

- Porous Explosive" *J. Appl. Physics*, Vol. 113, 194901, 2013.
4. Baer, M.R., "Modeling Heterogeneous Energetic Materials at the Mesoscale" *Thermochimica Acta*, Vol. 384, pp. 351-367, 2002.
 5. Yarrington, C.D., Wixom, R.R., and Damm, D.L., "Mesoscale Simulations Using Realistic Microstructure and First-Principles Equation of State" *Proc. of the JANNAF Winter meeting*, Monterey, CA, 2012.
 6. Wixom, R.R., et. al, "Characterization of Pore Morphology in Molecular Crystal Explosives by Focused Ion-beam nanotomography" *J. Mat. Res.*, Vol. 25, pp. 1362-1370, 2010.
 7. Wixom, R.R., "First-Principles Equations of State of Molecular Crystal Explosives" *Shock Compression of Condensed Matter*, Seattle, WA, July 2013.
 8. Rogers, R.N., "Thermochemistry of Explosives" *Thermochimica Acta*, Vol. 11, pp. 131-139, 1975.
 9. Kerley, G.I., "Theoretical Equations of State for the Detonation Products of Explosives" *Proc. of the 8th Detonation Symposium*, pp. 540-547, Albuquerque, NM, July 1985.
 10. Khasainov, B.A., Ermolaev, B.S., Presles, H.N., Vidal, P., "On the Effect of Grain Size on Shock Sensitivity of Heterogeneous High Explosives" *Shock Waves*, Vol. 7, pp. 89-105, 1997.
 11. Yarrington, C.D., Kittell, D., Wixom, R.R., Damm, D.L., "A Mie-Gruneisen EOS with Non-Constant Specific Heat" *Proc. of Shock Compression of Condensed Matter*, Seattle, WA, July 2013.
 12. Khasainov, B.A., Borisov, A.A., Ermolaev, B.S., Korotkov, A.I., "Two-Phase Visco-Plastic Model of Shock Initiation of Detonation in High Density Pressed Explosives" *Proc. of the 7th Detonation Symposium*, pp. 435-447, Annapolis, MD, June 1976.
 13. Tarver, C.M., Chidester, S.K., and Nichols A.L., "Critical Conditions for Impact- and Shock-Induced Hot Spots in Solid Explosives" *J. Phys. Chem.*, Vol. 100, pp. 5794-5799, 1996.
 14. Baer, M.R., Gartling, D.K., DesJardin, P.E., "Probabilistic Models for Reactive Behavior in Heterogeneous Condensed Phase Media" *Combust. Theory Modell.*, Vol. 16, pp. 75-106, 2012.
 15. Barua, A., Kim, S., Horie, Y., Zhou, M., "Prediction of probabilistic ignition behavior of polymer-bonded explosives from microstructural stochasticity" *J. Appl. Physics*, Vol. 113, 184907, 2013.
 16. Shan, R. et al., "Atomistic Simulation of Nanoscale Void-Enhanced Initiation in Hexanitrostilbene" *This Proceedings, 15th International Detonation Symposium*, San Francisco, CA, July 2014.
 17. Thompson, A. et al., "Micron-scale Reactive Atomistic Simulations of Void Collapse and Hotspot Growth in PETN" *This Proceedings, 15th International Detonation Symposium*, San Francisco, CA, July 2014.